ACS Photonics

pubs.acs.org/journal/apchd5

Article

Ultrafast Compressive Imaging of Neuronal Voltage Propagation Via a Slow Frame-Transfer Camera

Kelin Zhang, Shuzhang Liu, Peng Zou, and Jianglai Wu*

Cite This: ACS Photonics 2026, 13, 3419−3425

Read Online

ACCESS | Metrics & More | Article Recommendations | Supporting Information

ABSTRACT: Imaging ultrafast, faint biological events at microsecond resolution remains a significant challenge. Compressive sensing provides a promising framework to overcome the speed limitations, yet existing implementations are often hampered by complex hardware and insufficient sensitivity, severely restricting their utility in biological studies. Here, we introduce a compressive imaging technique that repurposes the intrinsic frame-transfer mechanism of a standard EMCCD camera to achieve ultrafast imaging beyond one million frames per second. Integrated seamlessly with a conventional fluorescence microscope, we demonstrate its capability by directly recording neuronal action potential propagation with microsecond resolution, showcasing its potential as a versatile and accessible tool for high-speed biological imaging.

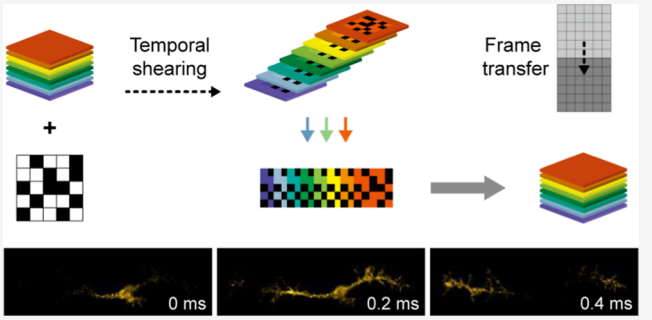

KEYWORDS: *ultrafast compressive imaging, neuronal voltage propagation, frame-transfer camera, snapshot compressive imaging, fluorescence voltage imaging*

INTRODUCTION

Direct visualization of propagating voltage signals in neurons is essential for unraveling the spatiotemporal dynamics of neural circuits, which is a cornerstone for understanding brain function and its neural basis in cognition and disease. Recent advances in fluorescence voltage indicators have enabled all-optical electrophysiology, offering a powerful paradigm for noninvasive monitoring of large neuronal populations.[1,2] However, the full potential of these indicators is constrained by the challenge of capturing their ultrafast fluorescence transient. Neuronal action potentials can travel at speeds over meters per second in the living brain, with the associated fluorescence transient lasting only microseconds.[3,4] This necessitates imaging systems with both high temporal resolution and high sensitivity to capture these faint and fleeting signals. While advanced high-speed cameras capable of capturing over one million frames per second are available, their speed typically comes at the expense of dynamic range and sensitivity, limiting their ability to detect faint fluorescence transients.[5] Consequently, existing methods often rely on slower but more sensitive cameras, estimating fast dynamics via frame interpolation based on known signal models.[2] Such inference-based strategies are inherently limited and can lead to a loss of information when imaging microsecond-scale voltage dynamics.

In recent years, snapshot compressive imaging (SCI) has emerged as a high-speed imaging technique capable of exceeding the native frame rate of conventional cameras.[6,7] In SCI, the temporally sheared and spatially encoded data cube (x, y, t) is projected onto a 2D sensor, from which high-speed image sequences are subsequently reconstructed from the compressed measurements. A variety of temporal shearing mechanisms have been employed, including external high-speed encoding devices such as piezoelectric stages, digital micromirror devices, and galvanometric scanners,[8−10] as well as intrinsic row-shift mechanisms found in cameras such as time-delay integration, rolling shutter, and streak cameras.[11−14] Notably, when combined with a streak camera, SCI can achieve temporal resolution in the picosecond regime, making it one of the fastest imaging modalities reported to date[15] and enabling ultrafast imaging applications once out of reach.[16−19] Nevertheless, existing platforms still lack the instrumental simplicity and sensitivity required for photon-starved applications, such as imaging fast and faint fluorescent transients in biological samples.

To address these challenges, we developed a minimalist ultrafast compressive imaging technique that leverages the inherent mechanism of a standard frame-transfer electron multiplying charge-coupled device (EMCCD) camera. Our

Received: March 4, 2026
Revised: May 28, 2026
Accepted: June 1, 2026
Published: June 8, 2026

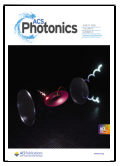

https://doi.org/10.1021/acsphotonics.6c00536
ACS Photonics 2026, 13, 3419−3425

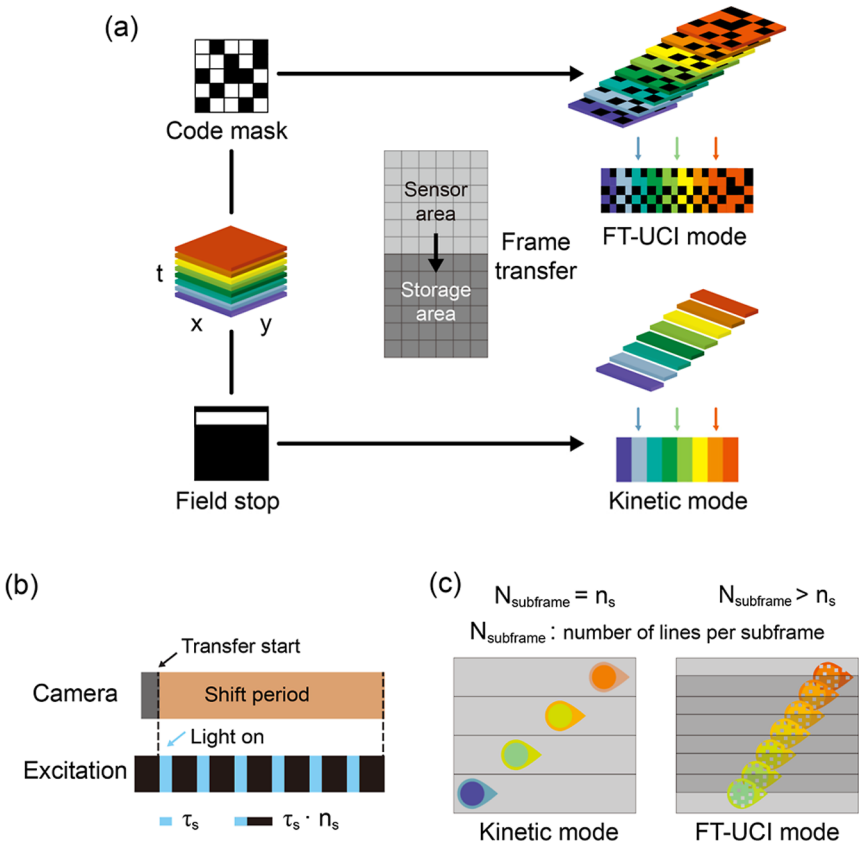

Figure 1. Working principle of the frame transfer-enabled ultrafast compressive imaging (FT-UCI). (a) Schematic comparison of standard kinetic and FT-UCI modes. (b) Timing diagram of frame transfer and exposure control. n_s, number of lines shifted between subframes; τ_s, line shift time. (c) Illustration of moving-object imaging in kinetic and FT-UCI modes.

core innovation lies in repurposing the camera's frame-transfer process as a precise, linear temporal shearing operator, granting our system the capability of microsecond resolution while eliminating the requirement for any external spatiotemporal modulation devices. By integrating our method seamlessly with a conventional fluorescence microscope, we harness the EMCCD's exceptional sensitivity to enable the visualization of action potential propagation with unprecedented temporal resolution, revealing fine temporal features of propagating signals that are difficult to resolve with conventional frame-limited imaging techniques.

RESULTS

Working Principle

The frame-transfer architecture in EMCCD cameras enables mechanical-shutterless imaging by quickly transferring the photon-generated charges within milliseconds from the photosensitive array to a shielded storage region, allowing continuous real-time image acquisition. In this work, we leverage this rapid transfer process to realize frame-transfer-enabled ultrafast compressive imaging (FT-UCI), operating under similar principles of snapshot compressive imaging[8] and compressed ultrafast photography.[14] During the frame transfer process, the spatially encoded three-dimensional scene (x-y-t) is temporally sheared and projected onto the two-dimensional sensor (Figure 1a). The entire process can be represented by a linear forward model: E = TSCI, where $I_{(x,y,t)}$ is the input dynamic scene, E represents the measured image, C denotes the spatial encoding operator, S represents the temporal shearing operator inherited from the frame-transfer process, and T is the spatiotemporal integration. Given prior knowledge of the operators, the original dynamic scene I can be computationally restored by solving the minimization problem of

$$\hat{I} = \arg\min\left\{\frac{1}{2}\|E-\mathrm{TSCI}\|_2^2 + \lambda\varphi(I)\right\} \quad (1)$$

in which λ and $\varphi(I)$ are the regularization parameter and function, respectively. To solve eq 1, we employ a generalized alternating projection-total variation algorithm, which has been widely used to reconstruct natural scenes in existing compressive imaging techniques.[20,21]

The frame rate of the FT-UCI microscope is given by $(n_s \times \tau_s)^{-1}$, where n_s is the number of lines shifted between subframes and τ_s is the line shift time (Figure 1b, c). During frame transfer, each subframe is illuminated by a light pulse with a duration $\leq \tau_s$ to mitigate interframe smearing. The EMCCD camera employed in this work (1024 × 1024, ProEM-HS, Teledyne) supports configurable line shift time τ_s of 0.7, 1.2, 2, or 5 μs. When operating at n_s = 1 and τ_s = 0.7 μs, the system achieves a maximum frame rate of 1.43 million frames per second (fps). Increasing n_s reduces the overlap between successive subframes, favoring higher-quality image reconstruction at the expense of temporal resolution. Notably, when subframes are fully transferred without spatial overlap (e.g., when the subframe line count equals n_s), the camera switches to the standard kinetic mode.[22] In this mode, it captures a sequence of discrete subframes at reduced speeds,

https://doi.org/10.1021/acsphotonics.6c00536
ACS Photonics 2026, 13, 3419−3425

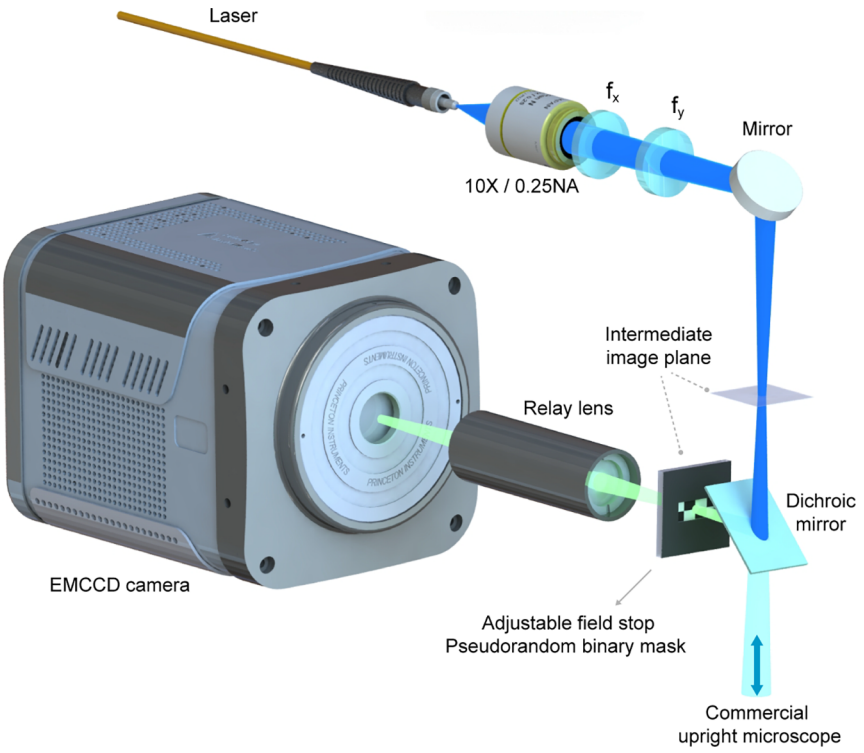

Figure 2. Schematic of the compressive ultrafast imaging microscope. f_x and f_y are x and y-focusing cylindrical lenses with focal lengths of 400 and 100 mm. In FT-UCI mode, a switchable binary mask is positioned at the intermediate plane for spatial encoding.

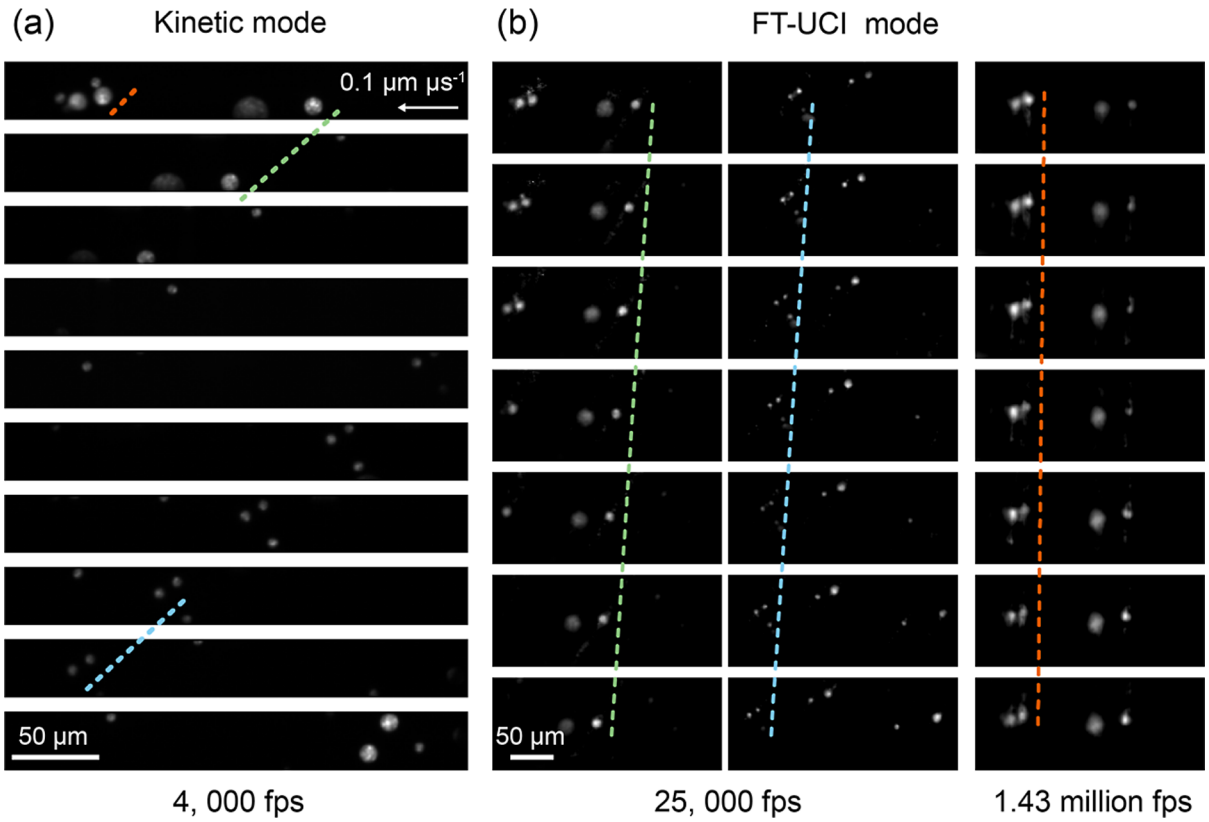

Figure 3. Fluorescent beads tracking with both FT-UCI and kinetic imaging modes. (a) Trajectories of moving beads captured in kinetic mode at 4, 000 fps. Images show 10 even-numbered frames out of a 20-frame sequence; frame-to-frame time interval, 500 μs. (b) Trajectories of the same beads captured in FT-UCI mode at 25, 000 fps (left) and 1.43 million fps (right); dashed lines indicate fine-scale trajectories at discontinuities highlighted in (a); images show 2- and 20-frame intervals (80 and 14 μs) extracted from 108- and 130-frame sequences, respectively. Laser intensity: 85 W cm^{-2} (pulse duration = τ_s) for all tests.

https://doi.org/10.1021/acsphotonics.6c00536
ACS Photonics 2026, 13, 3419−3425

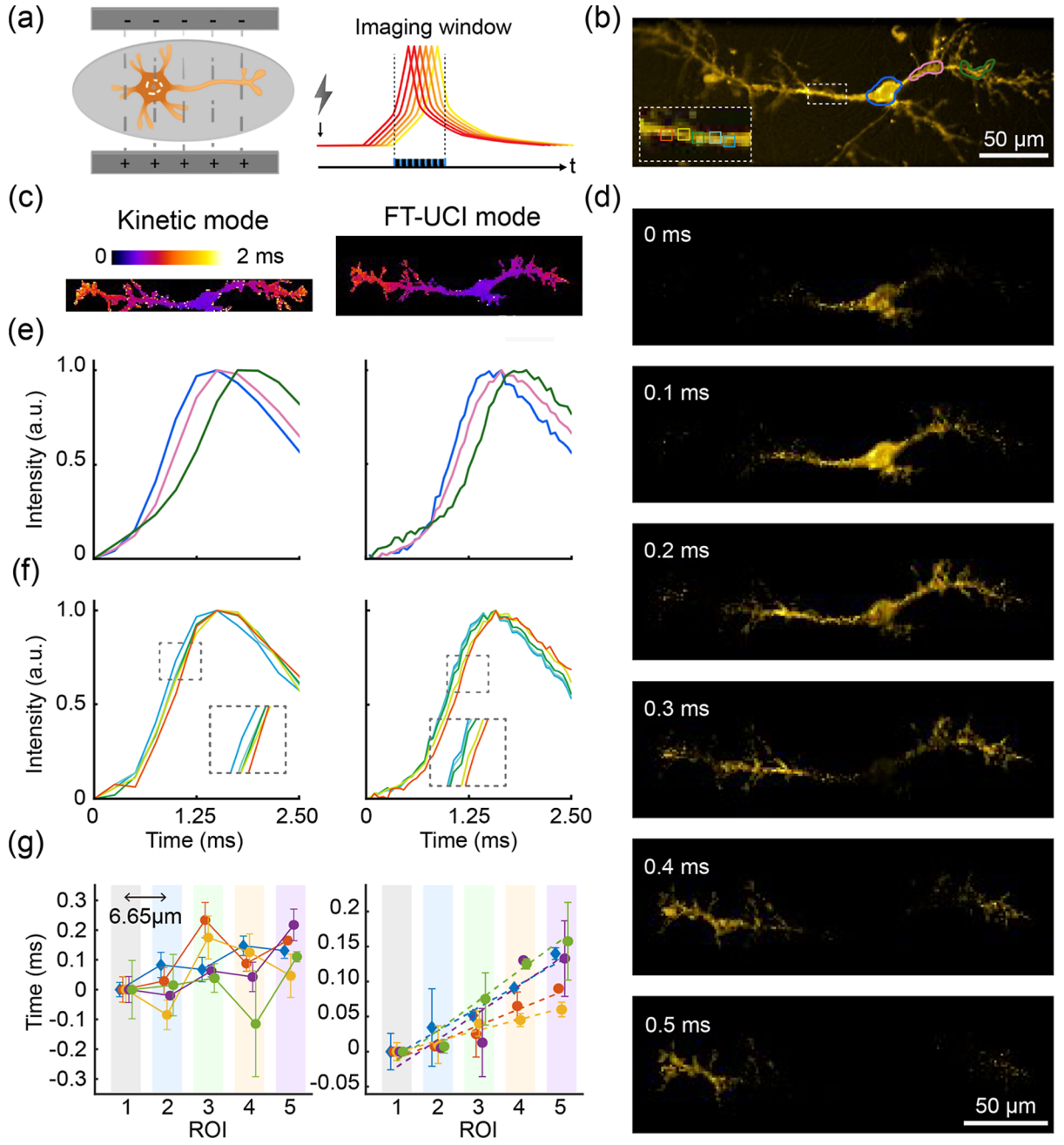

Figure 4. Ultrafast compressive imaging of action potential propagation. (a) Schematic of the extracellular field stimulation (40 V, 1.2 ms pulse; left) and corresponding imaging time diagram (right). (b) Widefield fluorescence image of a cultured neuron expressing HVI^{+}-Cy3b voltage indicator. (c) Action potential propagation time maps reconstructed from kinetic mode (4, 000 fps, left) and FT-UCI mode (20, 000 fps, right) recordings of the neuron shown in (b). (d) Selected frames from the action potential propagation movie reconstructed from the FT-UCI mode. (e) Voltage traces extracted from three colored ROIs in (b). (f) Voltage traces from five consecutive ROIs along the neurite (zoomed box in (b)), with the insets showing magnified rising phases. An average of 36 and 43 trails were used in FT-UCI and kinetic modes. (g) Timing of action potentials across the neurites in five neurons (mean ± SD, n = 5 tests). The ROIs were evenly distributed across the neurites. Data is shown for the neuron in (b) (diamonds) and four additional neurons (dots). Linear regression (dashed lines) indicates a propagation velocity of approximately 150−500 μm ms^{-1}. Laser intensity: 3, 500 W cm^{-2} (pulse duration = τ_s) for all tests.

eliminating the need for computational reconstruction (Figure 1a). The temporal imaging window, determined by the product of the number of transferable lines and line shift time, typically spans 1−5 ms, rendering it fit for imaging the dynamics of millisecond neuronal action potentials.

Experimental Setup

We implemented the ultrafast compressive imaging paradigm on an upright fluorescence microscope (BX53, Olympus) (Figure 2). The excitation source was a 532 nm continuous-wave laser (MLL-FN-532, CNI, Changchun). Its output was coupled to a Ø 200 μm, 0.22 NA multimode fiber for delivery. An embedded acousto-optic modulator with a 1 MHz analog bandwidth enables the laser to precisely tailor the illumination pulses for specific imaging. We shaped the fiber output using a pair of orthogonally oriented cylindrical lenses (LJ1567RM-A and LJ1363RM-A, Thorlabs). The resulting elliptical beam was

https://doi.org/10.1021/acsphotonics.6c00536
ACS Photonics 2026, 13, 3419−3425

subsequently focused through an objective lens (1.0 NA, XLUMPLFLN20XW, Olympus), producing a focal spot of ~222 μm × 56 μm. Fluorescence emission was reflected by a dichroic mirror (DMR-550SP, LBTEK), filtered by a long-pass filter (MEFH10-550SP, LBTEK), and finally projected onto the camera sensor by a 1:1 relay lens (TECHSPEC, Edmund). At the intermediate plane, an adjustable stop was used to define the effective field of view for both FT-UCI and kinetic modes. When operating in FT-UCI mode, a transmission pseudorandom binary mask was inserted into this plane to realize spatial encoding. To characterize the spatial resolution of the system, we imaged a USAF 1951 resolution target under FT-UCI mode; the microscope resolved the line patterns in Group 7, Element 6 (line width 2.19 μm) (Figure S1).

Experimental Demonstrations

We first imaged fast-moving fluorescent beads using the FT-UCI microscope. A mixture of fluorescent beads with diameters of 5, 10, and 20 μm was embedded in agarose and mounted on a motorized translational stage moving linearly at 0.1 μm μs^{-1}. Same beads can be imaged repetitively under both kinetic and FT-UCI modes. In kinetic mode, 20 frames were captured at 4, 000 fps (n_s = 50, τ_s = 5 μs; 400 × 50 pixels; Figure 3a). In FT-UCI mode, 108 and 130 frames were recorded and restored at 25, 000 fps (n_s = 8, τ_s = 5 μs; 400 × 160 pixels) and 1.43 million fps (n_s = 1, τ_s = 0.7 μs; 400 × 160 pixels), respectively (Figures 3b and S2). In both imaging modes, the short exposure time (τ_s) ensured motion artifact-free imaging. Because its frame rate was insufficient to fully sample the rapid movements, kinetic mode produced discontinuous trajectories. In contrast, compressive imaging mode achieved both higher frame rate and vertically expanded field coverages. This enhanced temporal sampling yielded smoother trajectories, demonstrating its capability for micro-second-resolution dynamic studies.

Next, we imaged action potential propagation in cultured rat hippocampal neurons expressing HVI^+-Cy3b voltage indicator.[23] Action potentials were evoked by field stimulation using a pair of platinum wire electrodes (1 mm diameter, 15 mm separation) positioned 2−3 mm above the cultured neurons, which were centered between the electrodes. Square pulses (45 V, 1.2 ms) were delivered by a stimulator triggered every 15 s via a digital delay generator, and neuronal activity was imaged using both kinetic and FT-UCI modes (Figure 4a). In kinetic mode, 20 frames were captured at 4, 000 fps (n_s = 25, τ_s = 10 μs; 190 × 25 pixels); in FT-UCI mode, 90 frames were recorded at 20, 000 fps (n_s = 5, τ_s = 10 μs; 190 × 62 pixels). Note that 2 × 2 hardware pixel binning was used to increase the signal-to-noise ratio, consequently doubling the line shift time and exposure time. Compressed images were robustly restored by the space- and intensity-constrained reconstruction framework with prior knowledge of neuronal morphologies.[24] Action potential timing (Figure 4b−d and Supporting Information Video) was estimated using the SNAPT algorithm developed to map voltage propagations from recordings at kilohertz frame rates.[2]

For large temporal delays across neuronal structures, both imaging modes achieved consistent voltage propagation characteristics, revealing a voltage propagation speed of 301 ± 53 μm ms^{-1} (mean ± SD, n = 6 neurons) in major neurites (Figure 4b, e), consistent with previous research.[25−27] We further examined voltage propagation along a ~27 μm-long neurite segment by analyzing the signal profiles from five consecutive regions of interest (ROIs) (Figure 4b, f). The action potential propagated across this segment in approximately 80 μs. As a result, kinetic mode failed to resolve fine-scale dynamics due to its constrained temporal resolution (250 μs frame time). In contrast, the 5-fold better temporal resolution in FT-UCI mode enabled more accurate temporal characterizations, retrieving naturalistic voltage dynamics (Figures 4f, g and S3). These observations underscore the efficacy of our microscope in studying rapidly propagating action potential, with potential applications including direct imaging of propagation along fast-conducting fibers and submillisecond electrical coupling via gap junctions.[28−31]

DISCUSSION AND CONCLUSION

In summary, we developed a minimalist compressive fluorescence microscope that exploits the frame transfer mechanism of a conventional EMCCD camera to enable ultrafast imaging exceeding one million frames per second. Our technique distinguishes itself from the state-of-the-art snapshot compressive imaging and compressed ultrafast photography platforms by generating the necessary temporal shearing through the camera's internal frame-transfer process. Rather than matching the extreme temporal resolution achievable with streak cameras, our approach strikes a practical balance between microsecond-scale temporal resolution and high sensitivity. Furthermore, it eliminates the need for external temporal-shearing devices, such as piezoelectric stages[8] or galvanometric mirrors.[10] The high sensitivity of the EMCCD camera also favors fluorescence imaging compared with snapshot compressive imaging that leverages conventional time-delay integration and sCMOS cameras.[11−13] Importantly, our technique remains compatible with standard fluorescence microscopes while offering system-level advantages, including a compact integrated architecture, simplified optical alignment, and the absence of mechanical moving components.

Our approach capitalizes on the EMCCD camera's intrinsic high sensitivity and dynamic range, which is essential for resolving ultrafast, weak fluorescence transients, such as the neuronal action potentials imaged. Furthermore, the electronic pixel shifts in frame transfer result in a linear and precisely controllable smearing process to shear the three-dimensional spatiotemporal data cube, thereby avoiding the nonlinear distortions that can occur with mechanical shearing strategies.[15] This inherent linearity significantly simplifies the reconstruction process, enabling high-fidelity imaging without additional postacquisition calibration associated with mechanically sheared systems.[32] The temporal resolution of the FT-UCI technique is limited by the camera's 0.7 μs minimum line shift time. Furthermore, the field of view is constrained by the number of transfer lines employed for temporal shearing, introducing a trade-off between temporal depth and spatial coverage. With the 1024 × 1024 sensor and the given line shift time, the achievable temporal depth is only a few milliseconds, making it insufficient for imaging longer transients. Improving the temporal resolution and depth would require a frame-transfer camera with a higher pixel count and faster line shift capabilities, which would correspondingly increase system cost.

While current mapping of voltage propagation requires multitrial averaging ($n \geq 5$) to enhance signal-to-noise ratio for accurate reconstruction (Figure S4 and Supporting Information Video), continuous advances in voltage indicators could enable reliable single-shot measurements—essential for capturing nonrepeatable dynamic events, such as stochastic neuro-

https://doi.org/10.1021/acsphotonics.6c00536
ACS Photonics 2026, 13, 3419−3425

transmitter release or spontaneous network bursting. We anticipate that our technique will enable new investigations of a wide range of fast biological processes at microsecond time scales.

■ ASSOCIATED CONTENT

Data Availability Statement

Data is available from the authors upon reasonable request.

Supporting Information

The Supporting Information is available free of charge at https://pubs.acs.org/doi/10.1021/acsphotonics.6c00536.

Visualization of action potential propagations in FT-UCI mode (AVI)

Spatial resolution characterization in FT-UCI mode; raw compressed image and reconstructed frames of moving fluorescent beads; action potential propagations captured in FT-UCI and kinetic modes; and comparison of single-shot and multiframe averaged reconstructions (PDF)

■ AUTHOR INFORMATION

Corresponding Author

Jianglai Wu − *Beijing Institute for Brain Research, Chinese Academy of Medical Sciences & Peking Union Medical College, Beijing 102206, China; Chinese Institute for Brain Research, Beijing 102206, China;* orcid.org/0000-0003-1153-6655; Email: wujianglai@cibr.ac.cn

Authors

Kelin Zhang − *College of Biological Sciences, China Agricultural University, Beijing 100193, China; Beijing Institute for Brain Research, Chinese Academy of Medical Sciences & Peking Union Medical College, Beijing 102206, China; Chinese Institute for Brain Research, Beijing 102206, China;* orcid.org/0009-0003-5111-0445

Shuzhang Liu − *College of Chemistry and Molecular Engineering, Peking University, Beijing 100871, China*

Peng Zou − *College of Chemistry and Molecular Engineering, Peking University, Beijing 100871, China;* orcid.org/0000-0002-9798-5242

Complete contact information is available at: https://pubs.acs.org/10.1021/acsphotonics.6c00536

Funding

This work was supported by the CAMS Innovation Fund for Medical Sciences (2024-I2M-3-024), the Beijing Municipal Science & Technology Commission (Z220009), and the startup funds from CIBR.

Notes

The authors declare no competing financial interest.

■ ACKNOWLEDGMENTS

We thank Woo-ping Ge Lab for the help on cell cultures and the CIBR Instrumentation Core for technical support.

■ REFERENCES

(1) Knöpfel, T.; Song, C. Optical voltage imaging in neurons: moving from technology development to practical tool. *Nat. Rev. Neurosci.* **2019**, *20* (12), 719−727.

(2) Hochbaum, D. R.; Zhao, Y.; Farhi, S. L.; Klapoetke, N.; Werley, C. A.; Kapoor, V.; Zou, P.; Kralj, J. M.; Maclaurin, D.; Smedemark-Margulies, N.; et al. All-optical electrophysiology in mammalian neurons using engineered microbial rhodopsins. *Nat. Methods* **2014**, *11* (8), 825−833.

(3) Foust, A.; Popovic, M.; Zecevic, D.; McCormick, D. A. Action potentials initiate in the axon initial segment and propagate through axon collaterals reliably in cerebellar purkinje neurons. *J. Neurosci.* **2010**, *30* (20), 6891−6902.

(4) Popovic, M. A.; Foust, A. J.; McCormick, D. A.; Zecevic, D. The spatio-temporal characteristics of action potential initiation in layer 5 pyramidal neurons: a voltage imaging study. *Journal of Physiology* **2011**, *589* (17), 4167−4187.

(5) Manin, J.; Skeen, S. A.; Pickett, L. M. Performance comparison of state-of-the-art high-speed video cameras for scientific applications. *Opt. Eng.* **2018**, *57* (12), 1.

(6) Yuan, X.; Brady, D. J.; Katsaggelos, A. K. Snapshot compressive imaging: theory, algorithms, and applications. *IEEE Signal Process. Mag.* **2021**, *38* (2), 65−88.

(7) Zhang, Z.; Zheng, S.; Qiu, M.; Situ, G.; Brady, D. J.; Dai, Q.; Suo, J.; Yuan, X. A decade review of video compressive sensing: a roadmap to practical applications. *Engineering* **2025**, *46* (3), 172−185.

(8) Llull, P.; Liao, X.; Yuan, X.; Yang, J.; Kittle, D.; Carin, L.; Sapiro, G.; Brady, D. J. Coded aperture compressive temporal imaging. *Opt. Express* **2013**, *21* (9), 10526−10545.

(9) Qiao, M.; Liu, X.; Yuan, X. Snapshot spatial−temporal compressive imaging. *Opt. Lett.* **2020**, *45* (7), 1659−1662.

(10) Liu, X.; Skripka, A.; Lai, Y.; Jiang, C.; Liu, J.; Vetrone, F.; Liang, J. Fast wide-field upconversion luminescence lifetime thermometry enabled by single-shot compressed ultrahigh-speed imaging. *Nat. Commun.* **2021**, *12* (1), 6401.

(11) Park, J.; Gao, L. Continuously streaming compressed high-speed photography using time delay integration. *Optica* **2021**, *8* (12), 1620−1623.

(12) Weinberg, G.; Katz, O. 100,000 frames-per-second compressive imaging with a conventional rolling-shutter camera by random point-spread-function engineering. *Opt. Express* **2020**, *28* (21), 30616−30625.

(13) Guzmán, F.; Meza, P.; Vera, E. Compressive temporal imaging using a rolling shutter camera array. *Opt. Express* **2021**, *29* (9), 12787−12800.

(14) Gao, L.; Liang, J.; Li, C.; Wang, L. V. Single-shot compressed ultrafast photography at one hundred billion frames per second. *Nature* **2014**, *516* (7529), 74−77.

(15) Lai, Y.; Marquez, M.; Liang, J. Tutorial on compressed ultrafast photography. *J. Biomed. Opt.* **2024**, *29* (S1), S11524.

(16) Qi, D.; Zhang, S.; Yang, C.; He, Y.; Cao, F.; Yao, J.; Ding, P.; Gao, L.; Jia, T.; Liang, J.; et al. Single-shot compressed ultrafast photography: a review. *Adv. Photonics* **2020**, *2* (01), 1.

(17) Wang, P.; Liang, J.; Wang, L. V. Single-shot ultrafast imaging attaining 70 trillion frames per second. *Nat. Commun.* **2020**, *11* (1), 2091.

(18) Liang, J.; Wang, P.; Zhu, L.; Wang, L. V. Single-shot stereo-polarimetric compressed ultrafast photography for light-speed observation of high-dimensional optical transients with picosecond resolution. *Nat. Commun.* **2020**, *11* (1), 5252.

(19) Kim, T.; Liang, J.; Zhu, L.; Wang, L. V. Picosecond-resolution phase-sensitive imaging of transparent objects in a single shot. *Sci. Adv.* **2020**, *6* (3), No. eaay6200.

(20) Yuan, X. Generalized alternating projection based total variation minimization for compressive sensing. In *2016 IEEE International Conference on Image Processing*; IEEE, 2016; 2539−2543.

(21) Lei, X.; Shahid, H.; Wu, S. A novel algorithm to improve image reconstruction quality for 2D streak camera. *Nucl. Instrum. Methods Phys. Res. Sect. A Accel. Spectrom. Detect. Assoc. Equip.* **2021**, *991*, 165023.

(22) Steves, M. A.; Xu, K. Direct microsecond wide-field single-molecule tracking and super-resolution mapping via CCD vertical shift. *Nat. Commun.* **2025**, *16* (1), 10503.

(23) Liu, S.; Ling, J.; Xie, B.; Zhang, Y.; Peng, L.; Yang, L.; Yu, Y.; Lin, J.; Tang, C.; Chen, Z.; et al. Positive-going hybrid indicators for voltage imaging in excitable cells and tissues. *Sci. Adv.* **2025**, *11* (32), No. eads1807.
(24) Zhu, L.; Chen, Y.; Liang, J.; Xu, Q.; Gao, L.; Ma, C.; Wang, L. V. Space- and intensity-constrained reconstruction for compressed ultrafast photography. *Optica* **2016**, *3* (7), 694−697.
(25) Bakkum, D. J.; Frey, U.; Radivojevic, M.; Russell, T. L.; Müller, J.; Fiscella, M.; Takahashi, H.; Hierlemann, A. Tracking axonal action potential propagation on a high-density microelectrode array across hundreds of sites. *Nat. Commun.* **2013**, *4* (1), 2181.
(26) Dworak, B. J.; Wheeler, B. C. Novel MEA platform with PDMS microtunnels enables the detection of action potential propagation from isolated axons in culture. *Lab Chip* **2009**, *9* (3), 404−410.
(27) Habibey, R.; Latifi, S.; Mousavi, H.; Pesce, M.; Arab-Tehrany, E.; Blau, A. A multielectrode array microchannel platform reveals both transient and slow changes in axonal conduction velocity. *Sci. Rep.* **2017**, *7* (1), 8558.
(28) Ni, Z.; Vial, F.; Avram, A. V.; Leodori, G.; Pajevic, S.; Basser, P. J.; Hallett, M. Measuring conduction velocity distributions in peripheral nerves using neurophysiological techniques. *Clin. Neurophysiol.* **2020**, *131* (7), 1581−1588.
(29) Seidl, A. H. Regulation of conduction time along axons. *Neuroscience* **2014**, *276*, 126−134.
(30) Dong, A.; Liu, S.; Li, Y. Gap junctions in the nervous system: probing functional connections using new imaging approaches. *Front. Cell. Neurosci.* **2018**, *12*, 320.
(31) Shimizu, K.; Stopfer, M. Gap junctions. *Curr. Biol.* **2013**, *23* (23), R1026−R1031.
(32) Marquez, M.; Lai, Y.; Liu, X.; Jiang, C.; Zhang, S.; Arguello, H.; Liang, J. Deep-learning supervised snapshot compressive imaging enabled by an end-to-end adaptive neural network. *IEEE J. Sel. Top. Signal Process.* **2022**, *16* (4), 688−699.

https://doi.org/10.1021/acsphotonics.6c00536
ACS Photonics 2026, 13, 3419−3425